Application of a Full Potential Method to Supersonic Aircraft Design and Analysis

Kenneth B. Walkley* and Gregory E. Smith†
Dynamic Engineering Incorporated, Newport News, Virginia

A method based on the conservation form of the full potential equation has been used to analyze realistic aircraft configurations at supersonic speeds. A fighter forebody with and without a canopy and a supersonic cruise wingbody concept have been addressed in the Mach 1.41–2.30 speed range. Comparisons of predicted and measured surface pressure distributions and lift and drag for the forebody configurations showed excellent to good correlations, although some oscillations in the computed pressures were observed. Good to excellent results for the wingbody configuration were obtained as well. The nonlinear behavior of the pitching moment was well predicted, although the magnitudes were somewhat low. These analyses have all been conducted using single-precision arithmetic on a 32-bit minicomputer. Execution times averaged 30–45 min for the forebody configurations and slightly over 4 h for the wingbody.

Nomenclature

C_D = drag coefficient
C_L = lift coefficient
C_P = pressure coefficient
C_m = pitching moment coefficient
l = length
M = freestream Mach number
x,y,z = Cartesian coordinates
α = angle of attack
γ = ratio of specific heats
ξ,η = curvilinear coordinates in circumferential and normal directions
ϕ = velocity potential

Subscripts

b = body
c = canopy
fric = skin friction
PL = canoy/forebody parting line
TCL = forebody top centerline

Introduction

LINEAR theory methods[1] have been widely used for many years in the aerodynamic design and analysis of slender supersonic configurations.[2,3] The application of these methods is relatively straightforward and the required computer resources are modest. As the design flight envelope of advanced fighter aircraft expands to include both efficient supersonic cruise and supersonic maneuver requirements, the linear theory methods become increasingly inappropriate tools for the aircraft designer. To estimate the aerodynamics of such vehicles more accurately, the designer must look to the nonlinear aerodynamic methodologies.

The nonlinear methodologies include methods based on the Navier-Stokes, Euler, and full potential equations. Due to computer limitations, the application of the full Navier-Stokes equations to arbitrary and complex geometries is not yet a practical reality, but significant progress has been made using the thin-layer approximation.[4] Euler solvers also require substantial computer resources and are somewhat restricted in the complexity of configurations that can be analyzed.[5] Impressive advances are being made, however, in the application of the Euler equations to practical problems in aircraft design[6] and combinations of Euler and linear theory methods have proved useful for designing a fighter aircraft wing.[7]

Techniques based on the full potential equation offer a very attractive alternative to the Euler equations approach. The full potential techniques are capable of providing results that are equivalent to the Euler results when the assumptions of irrotational and isentropic flow are valid. A significant reduction in computer resources also occurs when the full potential method is selected.

The purpose of this paper is to present and discuss the results of several analyses conducted using a full potential method.[8] Both pressure coefficient and force and moment coefficient comparisons with test results for several cases are included at supersonic Mach numbers of 1.41–2.30. Practical problems such as determining forebody aerodynamics with a high-visibility canopy or estimating the longitudinal aerodynamic characteristics of configurations with highly noncircular cross sections are addressed. Also included is a discussion of the efficiency of conducting analyses such as these on a computer system that is substantially less sophisticated than state-of-the-art supercomputers, but one that is widely available in government and industry facilities.

Methodology

The full potential methodology selected for the analyses presented in this paper is rapidly maturing to a level that meets the design and analysis tool characteristics described above. The method has been described in detail in a number of papers[8–12] and thus will only be summarized here.

The numerical method solves the full potential equation in conservation form for the supersonic flow past arbitrary and complex geometries. Configurations that can be treated may include a fuselage, canopy, wing, canard, nacelle, vertical and horizontal tails, and inlets. A flux-linearized upwind differencing technique is employed to advance the solution along the configuration. The finite-difference equations are solved using an implicit factorization scheme. Embedded subsonic regions are treated using conservative switching operators to transition from the supersonic marching algorithm to a subsonic relaxation technique. Computational grids between the body surface and a user-specified outer boundary are developed

Received Oct. 14, 1986; revision received May 15, 1988.
*Manager, Technology Group. Senior Member AIAA.
†Specialist Engineer, Analytical Aeronautics. Member AIAA.

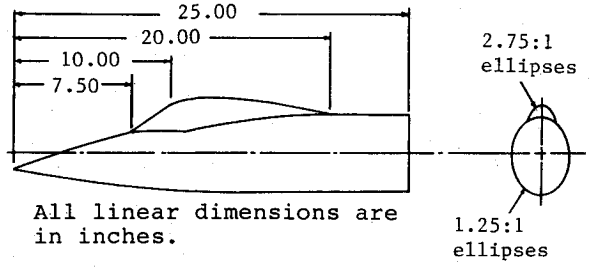

Fig. 1 Forebody configuration.

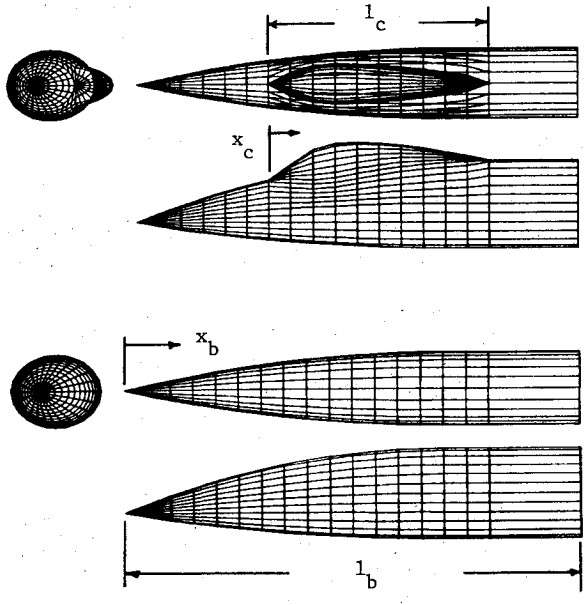

Fig. 2 Forebody wireframe representations with and without the canopy.

using an elliptic grid generation routine. Boundary conditions require no net normal flow at the body surface and freestream conditions at the outer boundary, which is set outside the bow shock location. A starting data plane is established near the nose of the configuration to initiate the solution. For sharp-nosed configurations, conical starting solutions are generated, while for blunt noses a method based on the axisymmetric unsteady full potential equation[13] is employed.

The geometry modeling requirements of this method are particularly attractive. Analytical descriptions of the configuration are not required. Instead, a surface description of a number of configuration cross sections is specified on a point-by-point basis. This type of geometry information is readily obtainable during the early stages of a configuration design and allows for efficient updates to the numerical model as the configuration is modified and refined. The cross-section defining points are splined by the code to obtain complete cross-section definitions, while linear interpolation is employed in the streamwise direction for marching plane locations between the input stations.

This full potential method solves the entire flowfield between the body surface and the outer boundary. Program output consists of velocity components and pressure coefficients at all grid points and overall force and moment components on the configuration.

The assumptions made in developing the full potential equation are somewhat restrictive, but nonetheless provide a useful flow model. At conditions where the product of the Mach number and local flow deflection exceed unity, however, the applicability of the full potential approach is no longer valid. This restriction, coupled with the requirement that the flow be irrotational, will limit the angle-of-attack and Mach number ranges that can be addressed. Similarly, when viscous effects predominate the flow or when flow separation is significant, the full potential model will not be adequate. In many other cases, it will be appropriate to estimate the skin-friction contribution using a separate methodology and add it to the inviscid drag predicted by the full potential method.

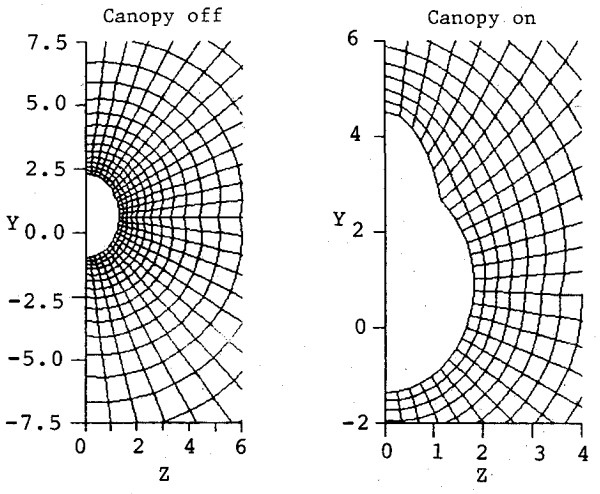

Fig. 3 Typical computational grids for the forebody.

Fighter Forebody Analysis

A fighter forebody with and without canopy for which experimental pressure and force data were available[14] was selected for analysis. Figure 1 illustrates the geometric details of the configuration with the canopy. Wireframe representations of the forebody alone and with the canopy in place are shown in Fig. 2. Test data were available for these two configurations at Mach numbers of 1.41 and 2.01 for angles of attack ranging from -6 to $+12$ deg. Although test results for nonzero sideslip angles are also available, only the zero sideslip cases were considered in the present analysis.

As noted in Fig. 1, both the forebody and canopy cross-sectional shapes are ellipses and thus the surface point definitions of the defining cross sections were easily and conveniently obtained from the equations for the ellipses. The line of intersection between the canopy and forebody (i.e., the parting line) was similarly determined.

A computational grid containing 20 points in the normal direction and 30 points in the circumferential direction (a 20×30 grid) was specified for the full potential code analyses. Typical grids for both configurations are shown in Fig. 3. Marching solutions for the forebody alone were obtained in a single program run, while three runs were required for the forebody with canopy — one for the forebody forward of the canopy, one for the canopy region, and one for the aft body. In each case, the marching step size was determined internally by the code based on CFL number considerations. The resulting number of marching planes for the forebody alone and for the forebody with canopy were 140 and 196, respectively.

Computed pressure distributions along the forebody top centerline at Mach 2.01 for angles of attack of 0.4, 6, and 12 deg are presented in Fig. 4. The full potential code results agree well with the data and accurately predict the variation in pressures associated with the angle-of-attack changes. Some irregularity in the computed pressure coefficients occurs near the nose, however, and at 12 deg angle of attack there is a lack of agreement with the test data over the rearward portion of the forebody where pressure values are more positive than the measured data.

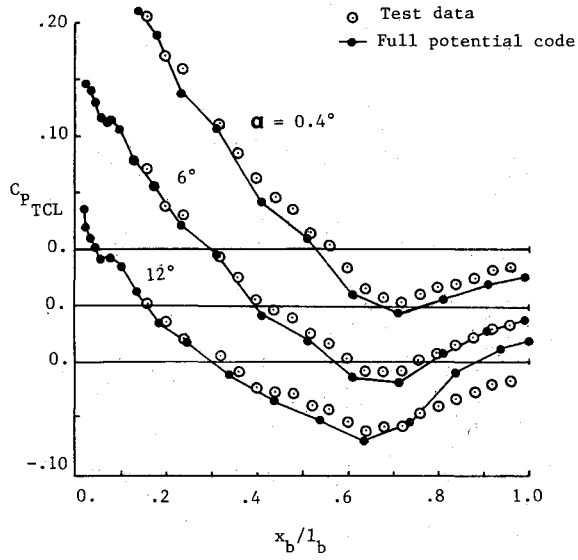

Fig. 4 Comparison of full potential code results and test data for the forebody alone at Mach 2.01.

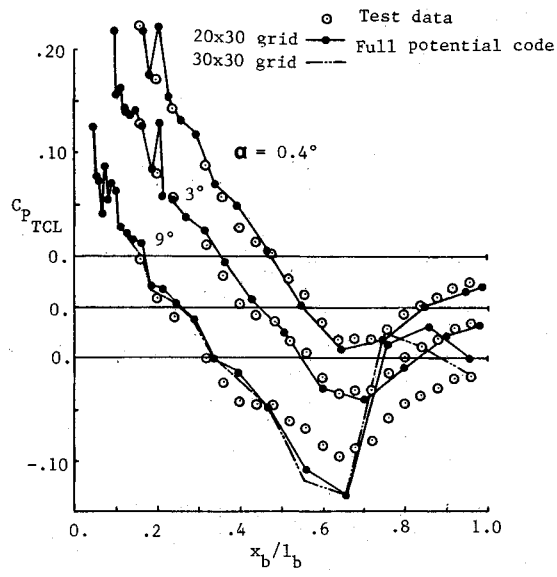

Fig. 5 Comparison of full potential code results and test data for the forebody alone at Mach 1.41.

Similar results are shown in Fig. 5 for a Mach number of 1.41 and angles of attack of 0.4, 3, and 9 deg. The full potential results agree quite well with the test data at $\alpha = 0.4$ and 3 deg. Accurate results were not obtained for the rear half of the forebody at the 9 deg angle of attack, however. For this case, the 20×30 grid was modified to a 30×30 grid to increase the normal grid density in an attempt to improve the computed results. As shown in Fig. 5, these results with the increased grid density are essentially the same as for the original 20×30 grid. At this combination of low Mach number and relatively high angle of attack, the code is apparently unable to properly handle the adverse pressure gradient along the lee side (top centerline) of the forebody. Decreasing the marching step size might improve the numerical results in this case.

As shown in Fig. 5, oscillations in the full potential code pressure distributions occur near the nose of the forebody. The reasons for these oscillations are, at present, not determined although they may be related to the transition from the conical starting solution to the nonconical marching technique. They do not appear to be related to a possible error in the input geometry as they occur at different longitudinal locations for the angles of attack considered. As will be shown, these oscillations have little effect on the computed force coefficients.

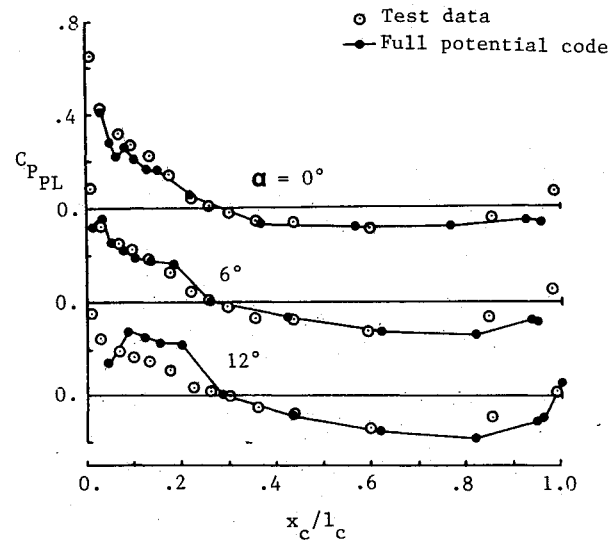

Fig. 6 Comparison of canopy/forebody parting-line pressures at Mach 2.01.

Comparisons of the measured pressure coefficients and the full potential code results for the forebody with canopy are shown in Fig. 6. Pressure coefficients along the canopy/forebody parting line (line of intersection) are plotted vs canopy fractional length for angles of attack of 0, 6, and 12 deg at Mach 2.01. In general, the full potential code results agree very well with the measured data. At 12 deg angle of attack, however, there is a sizable region over the forward 25% of the canopy where poor agreement between the computed and measured pressure coefficients occurs. This lack of agreement is most likely due to a local pocket of subsonic flow. A more detailed calculation for the subsonic pocket would probably improve these results. Also note that some oscillation occurs in the computed pressure distributions as has been described for the forebody alone.

Figures 7 and 8 summarize lift and drag coefficient results for the forebody alone. Similar results with the canopy are presented in Fig. 9. The full potential lift results agree very well with the measured data and accurately reflect the nonlinear characteristics. The drag correlation includes an estimate of the skin friction obtained using the T' method.[15] The full potential drag plus skin-friction results agree reasonably well with the measured data for the forebody alone at Mach 1.41, but uniformly underpredict the drag at Mach 2.01 for both configurations. This underprediction appears to be related to the skin-friction estimate. In particular, note that oscillations in the computed pressure distributions and local areas of disagreement between the measured and predicted pressures did not result in significant errors in the computed force coefficients.

Supersonic Cruise Configuration Analysis

Figure 10 illustrates a supersonic cruise wingbody configuration for which a set of both pressure data and force and moment data are available.[16,17] This Mach 3.0 design employs a modified arrow wing planform with a leading-edge sweep of 75 deg inboard and 60 deg in the wing tip region. A chine extends aft from the fuselage nose and blends into the wing leading edge at the wing side-of-body location. A minimum

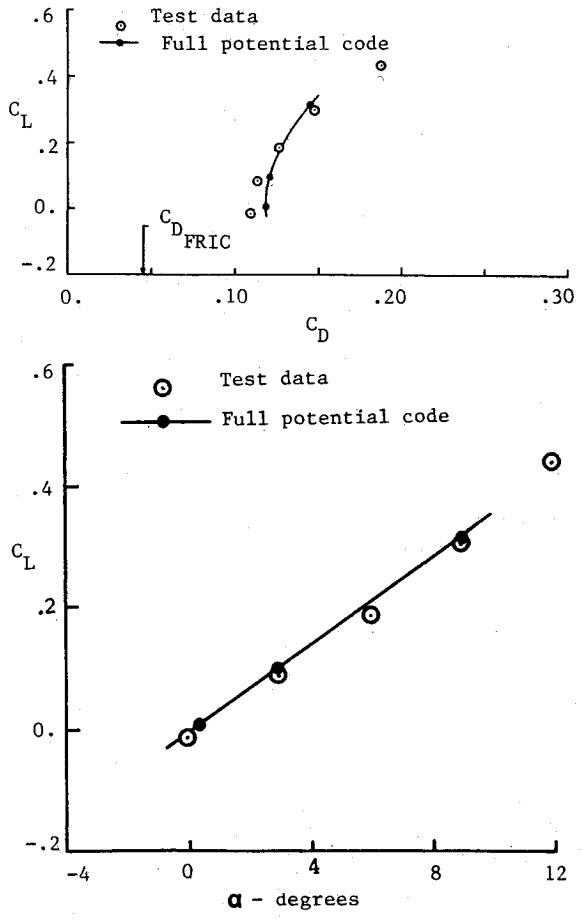

Fig. 7 Lift and drag results for the forebody alone at Mach 1.41.

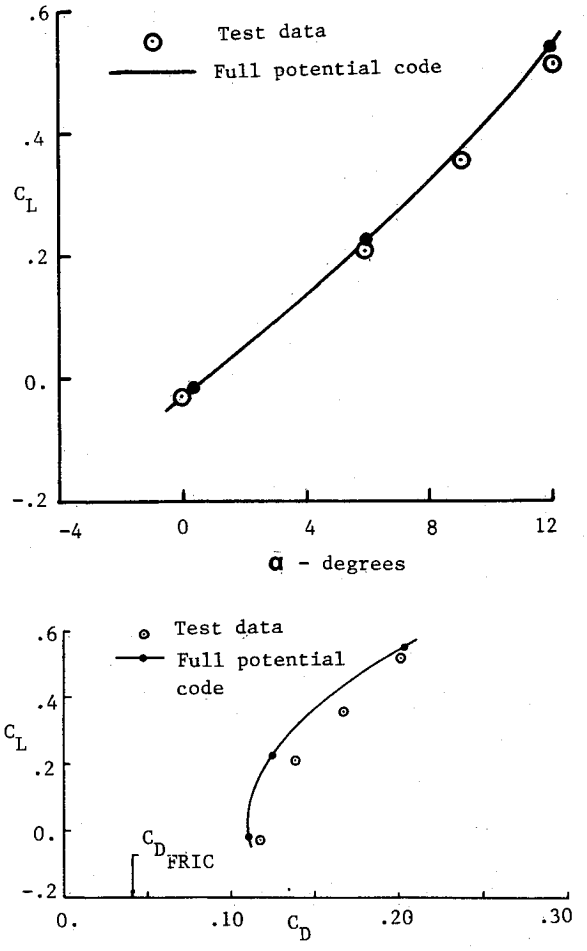

Fig. 8 Lift and drag results for the forebody alone at Mach 2.01.

drag wing twist and camber distribution is employed for improved supersonic performance.

The model geometry was measured on a three-axis dimension-recording machine to obtain accurate details of the model as tested. These measured geometric values were used to develop the numerical models for the full potential code analysis presented herein.

The full potential code has been used to analyze the wing-body combination at a Mach number of 2.3 and angles of attack of −0.18, 5.81, and 11.82 deg. Both pressure coefficient and force/moment coefficient correlations between the predicted and measured data have been made.

Typical computational grids for the cruise configuration are illustrated in Fig. 11. Grid densities ranged from 25 × 29 to 32 × 61 as the solution progressed down the length of the configuration. Grids were specified in two regions with the dividing line being the normal grid line that emerges from the wing tip. Approximately 400 marching planes were used over the length of the wingbody.

Comparisons of the computed and measured surface pressure distributions for the wingbody at Mach 2.3 for angles of attack of 5.80 and 11.82 deg are shown in Figs. 12 and 13. The cross-sectional locations selected for these comparisons correspond to those previously shown in Fig. 10.

At $\alpha = 5.81$ deg, the comparison between the predicted and measured results is excellent at station 25.53, but only fair at station 35.10. Although the lower surface pressures are well predicted at the more aft station, the upper surface values are more negative than the test data near the wing leading edge.

The agreement for $\alpha = 11.82$ deg is good to fair. At station 25.53 the predicted upper surface pressures are again too negative, while at station 35.10 the lower surface values are less positive than the measured data. The reasons for the lack of agreement between the predicted and measured pressures are

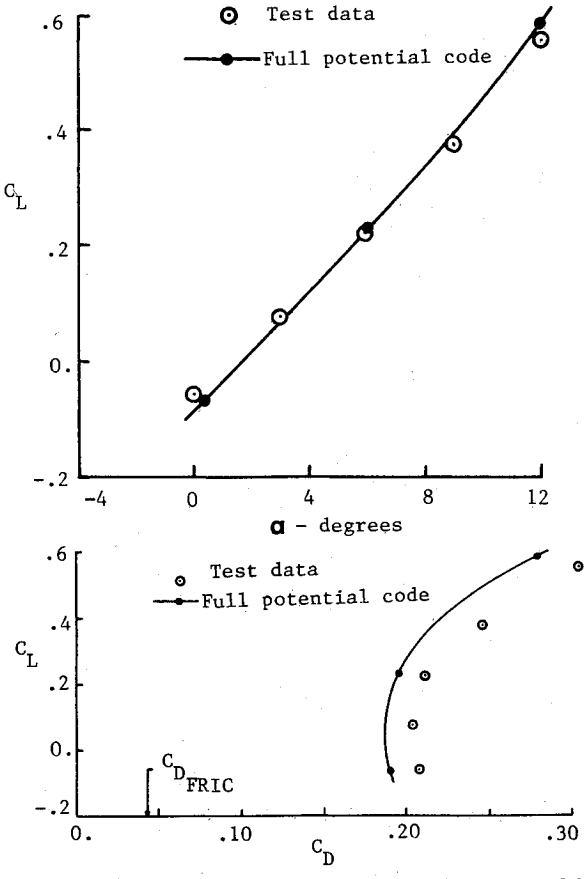

Fig. 9 Lift and drag results for the forebody and canopy at Mach 2.01.

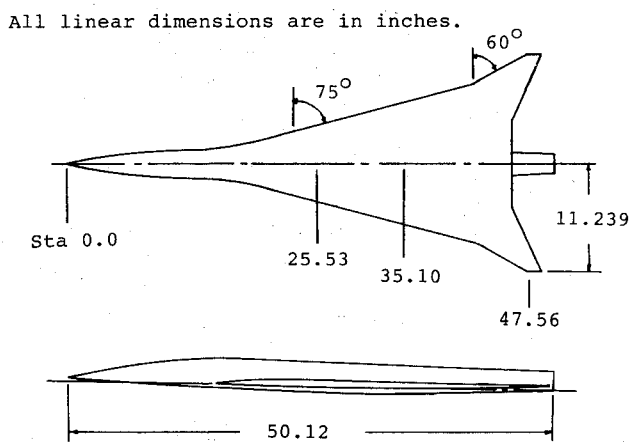

Fig. 10 Supersonic cruise configuration.

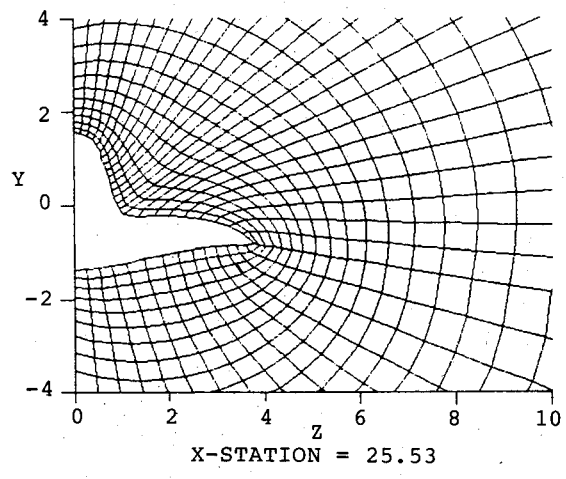

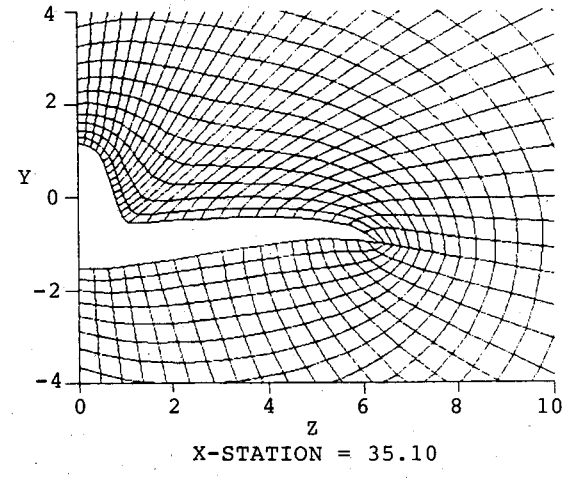

Fig. 11 Typical computational grids for the wing/body configuration.

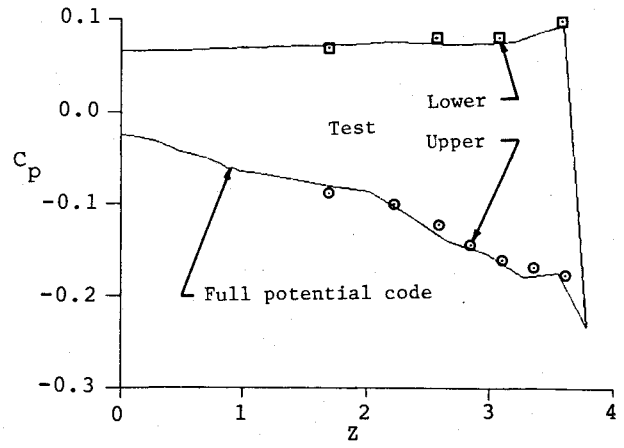

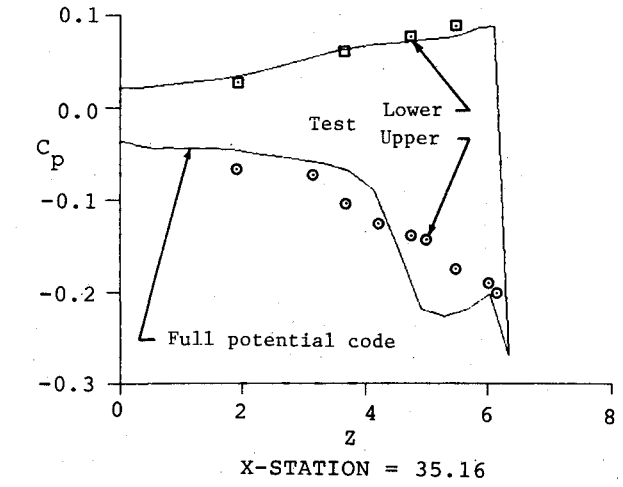

Fig. 12 Pressure coefficient profiles for the wing/body configuration at $\alpha = 5.81$ deg.

presumed to be related to the inability of the full potential method to model the vortex flows generated by the chine and highly swept wing leading edge. This vortex flow intensifies as the angle of attack increases, and the more aft longitudinal stations see a more fully developed vortex than do the forward stations.

The near-constant upper surface pressures shown in Fig. 13 for the outer portion of the wing reflect the pressure limiting incorporated into the full potential code. This feature prevents the computed pressures from exceeding the isentropic vacuum limit, $-2/\gamma M^2$. Pressure limiting is implemented through the density term in the full potential equation solution. This approach prevents numerical errors resulting from negative density values developed near the wing leading edge where the flow expands from the lower to the upper surface. As will subsequently be shown, these discrepancies in pressure coefficient result in relatively minor errors in the computed force coefficients.

Figure 14 illustrates the computational grid and pressure coefficient profile at station 47.56 where the wing wake is present along with the outboard wing panel. The angle of attack is 5.81 deg. The representation of wakes in the full potential code is done in an approximate manner. The full potential equation is not solved at wake points. Instead, the equation $\phi_{\eta\eta} = 0$ is solved such that the pressure change across the wake is approximately zero. The wake is thus a transparent surface through which flow may pass. As Fig. 14 shows, realistic wake characteristics can be obtained using this approach.

Lift results for the supersonic cruise wingbody configuration are presented in Fig. 15 for a Mach number of 2.3. The agreement between the predicted and measured data is excellent for the lift.

The T' method was used to estimate a skin-friction increment for the configuration. This result was combined with the pressure drag obtained from the full potential code to obtain the drag polar shown in Fig. 15. The agreement with the test data is excellent for lift coefficients up to about 0.15. Above this value, the agreement is good, although the drag is slightly underpredicted.

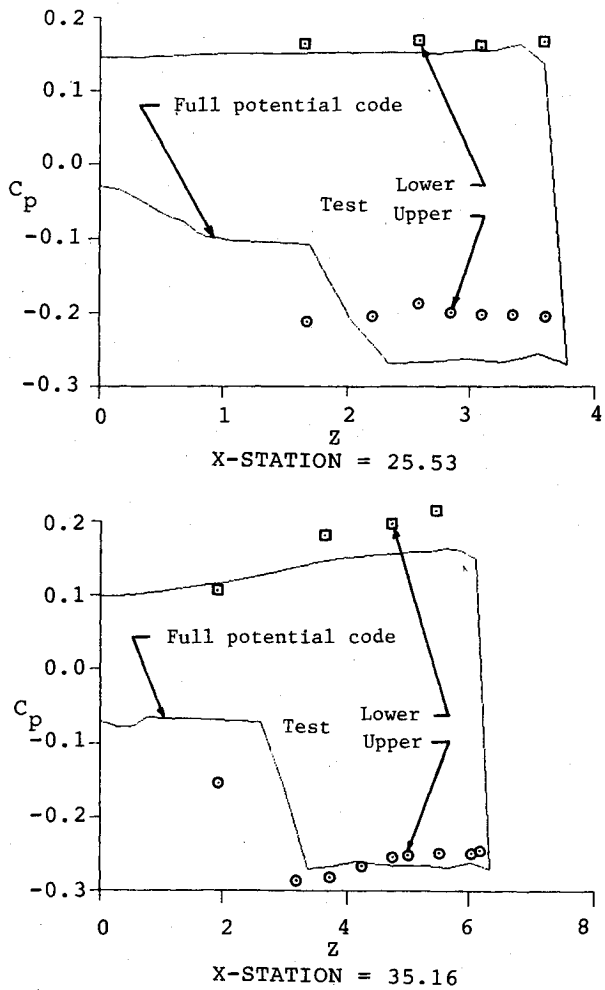

Fig. 13 Pressure coefficient profiles for the wing/body configuration at $\alpha = 11.82$ deg.

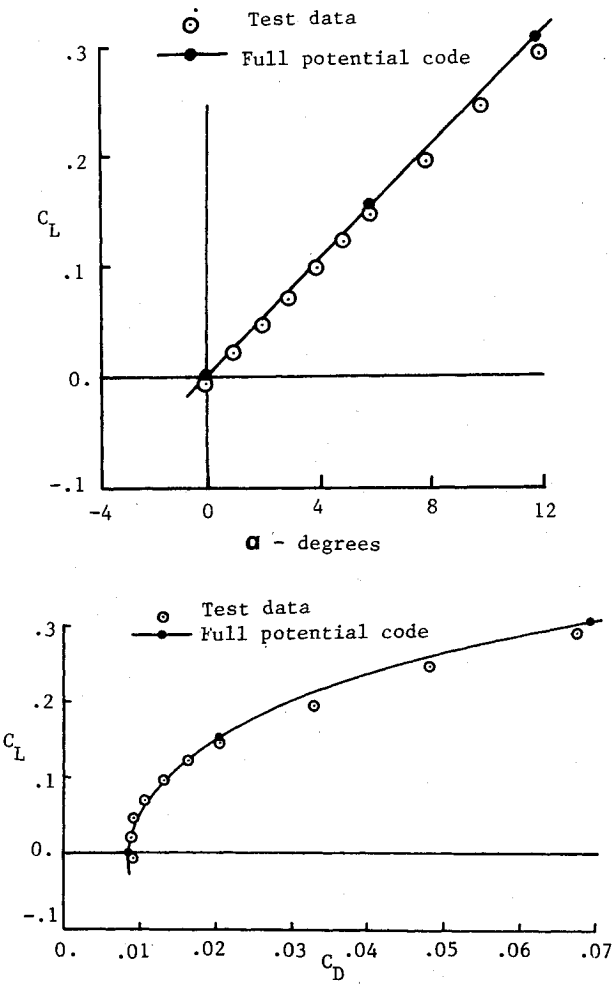

Fig. 15 Lift and drag coefficients for the wing/body configuration at Mach 2.30.

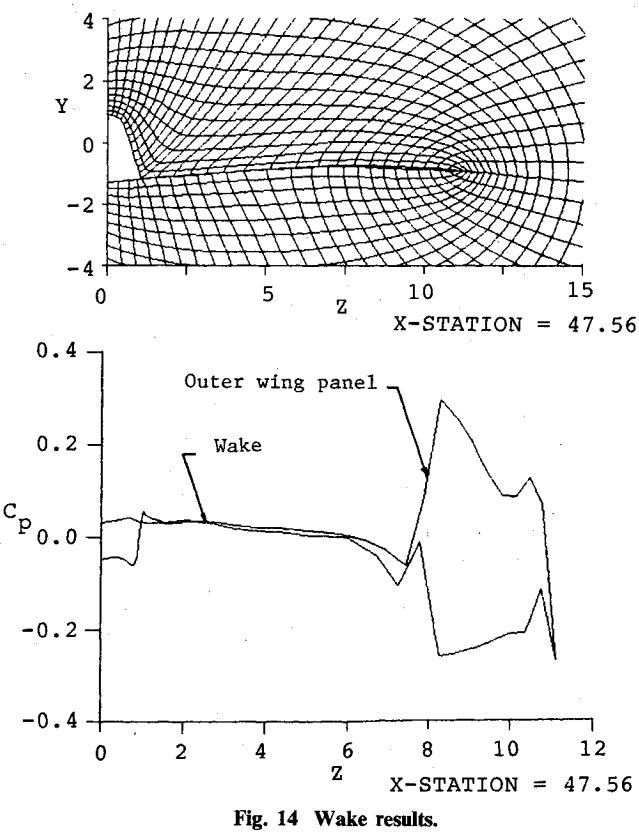

Fig. 14 Wake results.

Nonlinear pitching moment characteristics are particularly difficult to estimate accurately—especially at the higher angles of attack. As shown in Fig. 16, the full potential method predicts the trend of pitching moment with increasing lift coefficient, but fails to estimate the magnitude accurately. Errors in the computed pressures are evident in this case, even though compensating pressure errors probably contributed to the overall accuracy of the lift and drag predictions.

Overall, the full potential code has provided accurate estimates of both the aerodynamic loading and the longitudinal aerodynamic characteristics of the configuration.

Computer Considerations

These calculations were performed using single-precision (32 bit) arithmetic on a 1×10^6 instructions/s minicomputer. Execution times for each case ranged from 27 min for the forebody and 45 min for the forebody and canopy to 4 h, 11 min for the wingbody configuration.

Figure 17 illustrates the relative accuracy of single-precision vs double-precision arithmetic in executing the full potential code. The configuration selected for this analysis was the forebody alone at Mach 2.01 and 0.4 deg angle of attack. The computational grid in each case was 20×30. As the pressure distributions in the figure show, essentially identical numerical results were obtained in both cases. The double-precision case, however, required nearly twice the execution time. No code problems due to numerical precision were encountered in using the single-precision arithmetic.

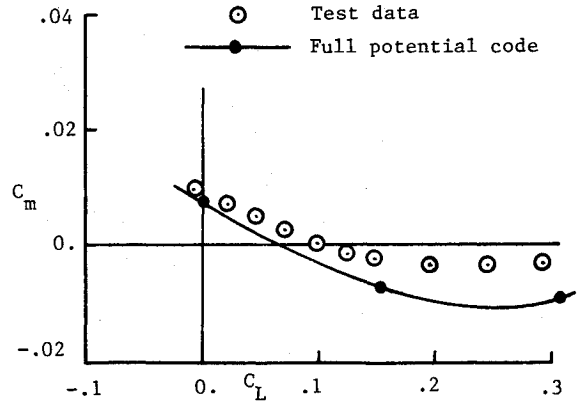

Fig. 16 Pitching moment coefficients for the wing/body configuration at Mach 2.30.

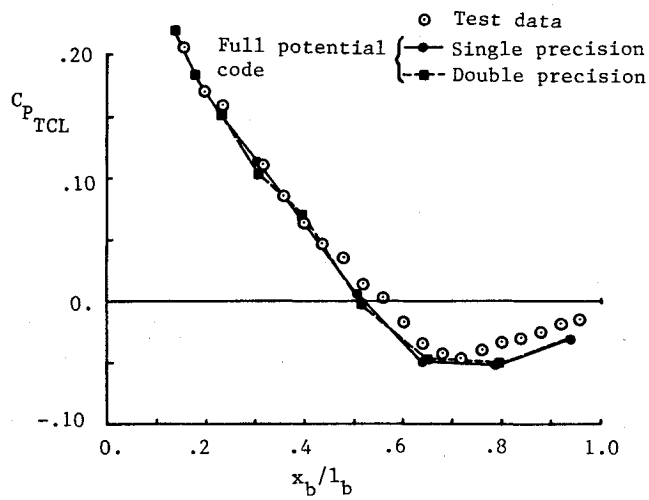

Fig. 17 Single- and double-precision full potential code results for the forebody alone (Mach 2.01, $\alpha = 0.4$ deg.).

Concluding Remarks

A method based on the conservation form of the full potential equation has been used to analyze realistic aircraft configurations at supersonic speeds. A fighter forebody with and without a canopy and a supersonic cruise wingbody configuration have been addressed in the Mach 1.41–2.3 speed range.

Predicted and measured surface pressures for the forebody agreed very well for angles of attack of 0–12 deg. Although oscillations in the computed pressure distributions were noted in some cases, the force coefficient correlations were good to excellent.

Good-to-excellent pressure distribution comparisons with wind-tunnel data for the supersonic cruise wingbody configuration were obtained as well. The overall lift and drag estimates were in excellent agreement with the test data. The nonlinear character of the pitching moment variation with lift coefficient was well predicted by the full potential code, although the estimated magnitudes were somewhat lower.

These analyses were conducted using single-precision arithmetic on a 32-bit virtual memory minicomputer. No numerical problems were evident in using the 32-bit arithmetic and the execution times were considerably faster than when using double precision. Forebody solutions required about 30–45 min of central processor time, while the wingbody runs averaged slightly over 4 h. These times are considered reasonable and acceptable for a widely available computer system that is reasonably inexpensive to obtain and operate.

The full potential code represents a useful and economical bridge between the linear theory and Euler methods. Further application and improvement of the method will result in a reliable design and analysis tool that can be confidently applied to a variety of supersonic problems.

Acknowledgment

This work was supported by the Directorate of Design Analysis, Deputy for Development Planning, Aeronautical Systems Division, Air Force Systems Command, Wright-Patterson Air Force Base, Ohio, under Contract F33615-83-0130, Task 0130-26.

References

[1]Middleton, W. D. and Lundry, J. L., "A System for Aerodynamic Design and Analysis of Supersonic Aircraft, Part 1: General Description and Theoretical Development," NASA CR 3351, 1980.

[2]Baals, D. D., Robins, A. W., and Harris, R. V., Jr., "Aerodynamic Design Integration of Supersonic Aircraft," AIAA Paper 68-1018, 1968.

[3]Walkley, K. B. and Martin, G. L., "Aerodynamic Design and Analysis of the AST-200 Supersonic Transport Configuration Concept," NASA CR 159051, 1979.

[4]Rizk, Y. M. and Ben-Shmuel, S., "Computation of the Viscous Flow Around the Shuttle Orbiter at Low Supersonic Speeds," AIAA Paper 85-0168, 1985.

[5]Moitra, A., "Numerical Solution of the Euler Equations for High-Speed, Blended Wing-Body Configurations," AIAA Paper 85-0123, 1985.

[6]Chakravarthy, S. R. and Szema, K. Y., "An Euler Solver for Three-Dimensional Supersonic Flows with Subsonic Pockets," AIAA Paper 85-1703, 1985.

[7]Ross, J. M., Reaser, J. S., and Bouchard, E. E., "Optimization of a Supersonic Wing by Combining Linear and Euler Methods," Society of Automotive Engineers Paper 851791, 1985.

[8]Shankar, V., Szema, K. Y., and Bonner, E., "Full Potential Methods for Analysis/Design of Complex Aerospace Configurations," NASA CR 3982, 1986.

[9]Shankar, V., "Conservative Full Potential, Implicit Marching Scheme for Supersonic Flows," *AIAA Journal*, Vol. 20, Nov. 1982.

[10]Shankar, V. and Osher, S., "An Efficient Full-Potential Implicit Method Based on Characteristics for Supersonic Flows," *AIAA Journal*, Vol. 21, Sept. 1983.

[11]Shankar, V., Szema, K. Y., and Osher, S., "Treatment of Supersonic Flows with Embedded Subsonic Regions," *AIAA Journal*, Vol. 23, Jan 1985.

[12]Szema, K. Y., Riba, W. L., Shankar, V., and Gorski, J. J., "Computation of Supersonic Flows over Three-Dimensional Configurations," *Journal of Aircraft*, Vol. 22 , Dec. 1985, pp. 1079–1084.

[13]Shankar, V., Ide, H., and Gorski, J., "Relaxation and Approximate Factorization Methods for the Unsteady Full Potential Equation," Paper ICAS-84-1.6.2, Sept. 1984.

[14]Robins, A. W., "Force and Pressure Measurements on Several Canopy-Fuselage Configurations at Mach Numbers 1.41 and 2.01," NACA RM L55H23, 1955.

[15]Sommer, S. C. and Short, B. J., "Free-Flight Measurements of Turbulent-Boundary-Layer Skin Friction in the Presence of Severe Aerodynamic Heating at Mach Numbers from 2.8 to 7.0," NACA TN 3391, 1955.

[16]Shrout, B. L. and Fournier, R. H., "Aerodynamic Characteristics of a Supersonic Cruise Airplane Configuration at Mach Numbers of 2.30, 2.96, and 3.30," NASA TM 78792, 1979.

[17]Shrout, B. L., Corlett, W. A., and Collins, I. K., "Surface Pressure Data for a Supersonic-Cruise Airplane Configuration at Mach Numbers of 2.30, 2.96, and 3.30," NASA TM 80061, 1979.